ACS APPLIED NANO MATERIALS
Cite This: ACS Appl. Nano Mater. 2019, 2, 3695−3700
Article
www.acsanm.org

Pd@Pt Core−Shell Nanodots Arrays for Efficient Electrocatalytic Oxygen Reduction

Shuo Li, Jiawei Liu, Guilin Zhu, and Heyou Han*

State Key Laboratory of Agricultural Microbiology, College of Science, Huazhong Agricultural University, No. 1, Shizishan Street, Hongshan District, Wuhan 430070, China

Supporting Information

ABSTRACT: Conformal deposition of Pt-dots arrays on polyhedral Pd nanocrystals can enhance Pt catalytic properties and reduce its loading. Herein, a simple method for the fabrication of Pd@Pt core−shell nanodot arrays (Pd@PtNAs) heterostructures via reducing H_2PtCl_6 and Na_2PdCl_4 by L-ascorbic acid in an aqueous solution with cetylpyridinium chloride and KBr is reported. The Pt nanodots arrays with a small size (about 3 nm in diameter) were dispersed on the surface of Pd decahedra. Such ultrasmall size Pt dots arrays can effectively increase the proportion of low-coordination Pt atoms. Compared with commercially available Pt/C catalysts, the Pd@PtNAs show obvious improvement in catalytic performance applied to oxygen reduction reaction. The mass activity (0.20 A/mg_{Pt}) of the obtained Pd@PtNAs with 36.9 wt % Pt shows 2.2 times relative to Pt/C catalyst (0.09 A/mg_{Pt}) for ORR. What's more, the Pd@PtNAs with 36.9 wt % Pt exhibited highly stable property and mass activity with only 11% loss after 10 000 testing cycle.

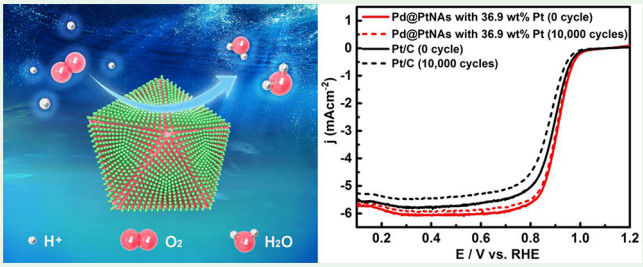

KEYWORDS: *Pd decahedra, Pt nanodots arrays, oxygen reduction reaction, ultrasmall size, heterostructures*

1. INTRODUCTION

Proton exchange membrane fuel cell (PEMFC) can efficiently convert chemical energy to electrical power under high power density with zero emission, which is considered to be one of the most important technologies to replace the existing nonregenerated energy resources.[1,2] The Pt-based nanomaterials have been widely used as cathode/anode catalysts for PEMFC, including oxygen reduction reaction (ORR) and oxidation of alcohols or hydrogen.[3−5] However, the application and development of PEMFC are extremely restricted due to the costly price of Pt.[6−10] Making full use of Pt atoms in Pt nanomaterials is an effective way to solve this problem.[11] Therefore, many specific structures of Pt-based nanocatalysts have been developed to raise the catalytic activity of ORR and oxidation of alcohols by regulating their morphology, size, and composition.[12−16] Deposition of Pt onto other metallic nanocrystals to form ultrathin layers or multibranched structures is proven to be an effective method.

The core−shell and/or bimetallic heterostructures have been explored as the highly active structures to enhance the activity.[17−22] The Xia group has reported a series of Pd@Pt core−shell nanomaterials synthesized by depositing a single layer or several layers of Pt atoms onto Pd nanocrystals with an octahedral,[23−25] decahedral,[26] cubic,[27] or icosahedral[28,29] shape. In addition, Pd−Pt nanodendrites have been prepared by depositing Pt branch on Pd nanocrystals using seeded-growth methods or one-pot synthesis.[22,30−32] Compared with commercialized Pt/C catalyst, such catalysts showed remarkable enhancement in activity and durability. However, Pt-on-Pd nanodot arrays formed by depositing ultrasmall size Pt nanodots on Pd nanocrystals are rarely reported.

Herein, we report a simple method to obtain Pd@Pt core−shell nanodots arrays heterostructures by reducing Na_2PdCl_4 and H_2PtCl_6 with L-ascorbic acid (AA) in an aqueous solution with cetylpyridinium chloride (CPC) and KBr. The Pt nanodot arrays with a small size (about 3 nm in diameter) were dispersed on the surface of Pd decahedra. Such ultrasmall size Pt dots arrays can effectively increase the proportion of Pt atoms.[10,33,34] The arrays of Pt dots can effectively prevent the sintering and agglomeration of Pt materials in the process of electrocatalysis.[35,36] Compared with commercially available Pt/C catalysts, the catalytic performance of Pd@PtNAs for ORR have been improved.

2. EXPERIMENTAL SECTION

2.1. Reagents and Materials. Hexachloroplatinic acid hexahydrate ($H_2PtCl_6·6H_2O$, AR), L-ascorbic acid (AA, AR), perchloric acid ($HClO_4$, 70.0−72.0%), and potassium bromide (KBr, AR) were bought from the Sinopharm Chemical Reagent Co., Ltd. Cetylpyridinium chloride (CPC, 98.0%) and sodium tetrachloropalladate (Na_2PdCl_4, 98.0%) were bought from Aladdin Chemical Reagent Company. Commercial Pt/C (20 wt % of Pt) was bought from Alfa Aesar Chemicals Co., Ltd. Nafion perfluorinated resin solution (5 wt %) was purchased by Sigma-Aldrich. Ultrapure water with the resistance of 18.2 MΩ/cm was utilized in all experiments.

Received: April 2, 2019
Accepted: May 15, 2019
Published: May 15, 2019

DOI: 10.1021/acsanm.9b00610
ACS Appl. Nano Mater. 2019, 2, 3695−3700

2.2. Synthesis of Pd Decahedra. In a typical synthesis, 0.04 g of CPC, 0.02 g of KBr, and 0.04 g of AA were dissolved into 4 mL of water. After stirring for 5 min at room temperature, 100 μL of Na_2PdCl_4 (34 mM) were added into the above mixture solution, followed by stirring for 1 h at 100 °C. The brownish black product was collected by centrifugation (13 500 rpm, 8 min) and washed twice with ethanol and water, repsectively, to remove residual CPC and KBr. The final product was redispersed into 200 μL of water.

2.3. Synthesis of Pd@PtNAs. The synthesis method of Pd@PtNAs was similar to that of Pd decahedra except that 88 μL (or 176 μL) of H_2PtCl_6 (20 mM) was added.

2.4. Material Characterizations. The morphology and structure characterization of Pd@PtNAs were conducted via transmission electron microscope (TEM, JEM-2010FEF, 80 kV) and high-resolution TEM (HRTEM, Tecnai G2 F30, 200 kV) with a selected-area electron diffraction (SAED) accessory. The element composition of Pd@PtNAs was analyzed by high-angle annular dark-field scanning transmission electron microscope (HAADF-STEM, JEM-ARM 200F, 200 kV) with energy-dispersive X-ray spectroscopy (EDS). The crystal structure of Pd@PtNAs was conducted by X-ray diffraction (XRD, Bruker D8 Advance). The precise composition of Pd@PtNAs was tested by inductively coupled plasma mass spectrometry (ICP-MS, PerkinElmer NexION 300Q).

2.5. Electrochemical Measurements. A three electrodes electrochemical system with a working electrode (glassy carbon electrode, 0.196 cm^2), a counter electrode (platinum wire), and a reference electrode (Ag/AgCl, saturated KCl) was operated in all electrochemical experiments. The electrochemical workstation (CHI 660B, Chenhua Co., Shanghai, China) with rotating disk electrode (RDE, Pine AFMSRCE) was used for electrochemical measurements. Cyclic voltammetry (CV) test was performed from −0.2 to 1.0 V (V versus Ag/AgCl) in N_2-saturated $HClO_4$ solution (0.1 M) with a sweep rate of 50 mV/s at 25 °C. The ORR polarization curve was acquired from −0.2 to 0.95 V (V versus Ag/AgCl) in O_2-purged $HClO_4$ solution (0.1 M) with a sweep rate of 10 mV/s and a certain rotation rate (1 600 rpm) at 25 °C.

3. RESULTS AND DISCUSSION

Pd@PtNAs were synthesized by the one-step hydrothermal reduction of Na_2PdCl_4 and H_2PtCl_6 utilizing L-ascorbic acid as reducing agent, CPC as the stabilizing agent, and KBr as the primary crystal-regulating agent. When the reaction starts, the generated Pd atoms will congregate to clusters and then grow to Pd decahedra particles under the coregulation of CPC and KBr.[37,38] As the reaction continues, the Pt atoms further grew to dot arrays deposited on the Pd decahedral surface as schematically illustrated in Scheme 1A.

The Volmer—Weber (VW) growth mode would occur immediately after the formation of Pd decanedron nanoparticles. Scheme 1B describes the major steps for the synthesis of Pd@Pt. As the surface free energy of Pt (γPt) is higher than Pd (γPd), the overall excess free energy ΔG is positive during the sedimentary growth process of Pt nanoparticles on the surface of Pd decahedra.[6] The subsequently formed Pt atoms would be grown epitaxially on the Pd decahedra surface, thus generating Pt particle array in the presence of CPC.[37] Figure S1 shows the TEM image of the Pd decahedra with a smooth surface. As shown in Figure S2, Pt nanoparticles cannot be obtained without Pd precursor. However, the Pd@PtNAs structures in Figure 1 performed with the Pd and Pt precursor in the reaction solution, which revealed that initially formed Pd decahedra acted as seeds for the subsequent growth of Pt nanodots.[31]

Scheme 1. Schematic Illustrations[a]

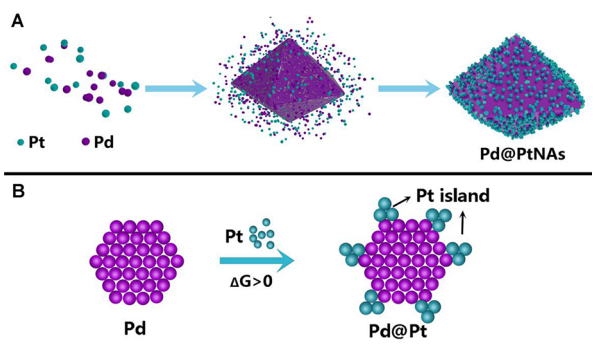

[a]Schematic illustrations for the synthesis (A) and formation mechanism (B) of Pd@PtNAs.

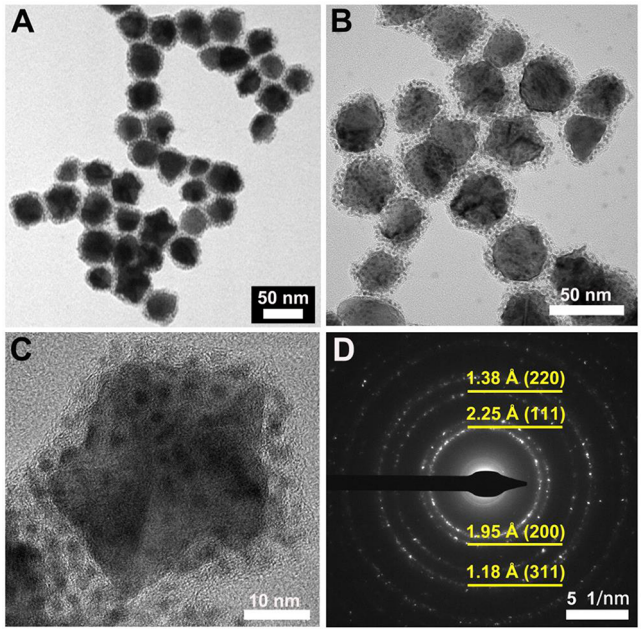

Figure 1. Structural and morphological analyses of the Pd@PtNAs with 36.9 wt % Pt. (A,B) TEM images. (C) HRTEM image. (D) SAED pattern.

Figure 1A,B shows the TEM image of the Pd@PtNAs with the sizes of 40−50 nm by adding 88 μL H_2PtCl_6 (20 mM) solution in the reaction system. The wt % (mass fraction) of Pt in this sample was 36.9% by ICP-MS analysis (Table S1). The microstructure of Pd@PtNAs was further characterized by HRTEM. Through the HRTEM image, we found that many nanodots with an average size of 3 nm forming nanodots arrays were dispersed on the surface of decahedra (Figure 1C). The SAED pattern showed that Pd@PtNAs had a representative of lattice plane with an interplanar distance of about 2.25 and 1.95 Å, which were considered as the characteristic (111) and (200) plane of Pd with face-centered cubic (fcc) structure (Figure 1D).[9,31] The lattice distance of Pt dots were 0.22 and 0.19 nm, which also attests the (111) and (200) for the fcc metallic Pt (Figure S3). From the XRD spectrum (Figure S4), the diffraction peaks can be well identified to the characteristic peaks of (111), (200), (220), and (311) facets of Pd and Pt with fcc structure (Joint Committee on Powder Diffraction Standards (JCPDS) number: 46-1043 and 04-0802 respectively).[39]

The HAADF-STEM image shown in Figure 2A revealed that nanodots arrays with an average diameter size of 3 nm were

DOI: 10.1021/acsanm.9b00610
ACS Appl. Nano Mater. 2019, 2, 3695−3700

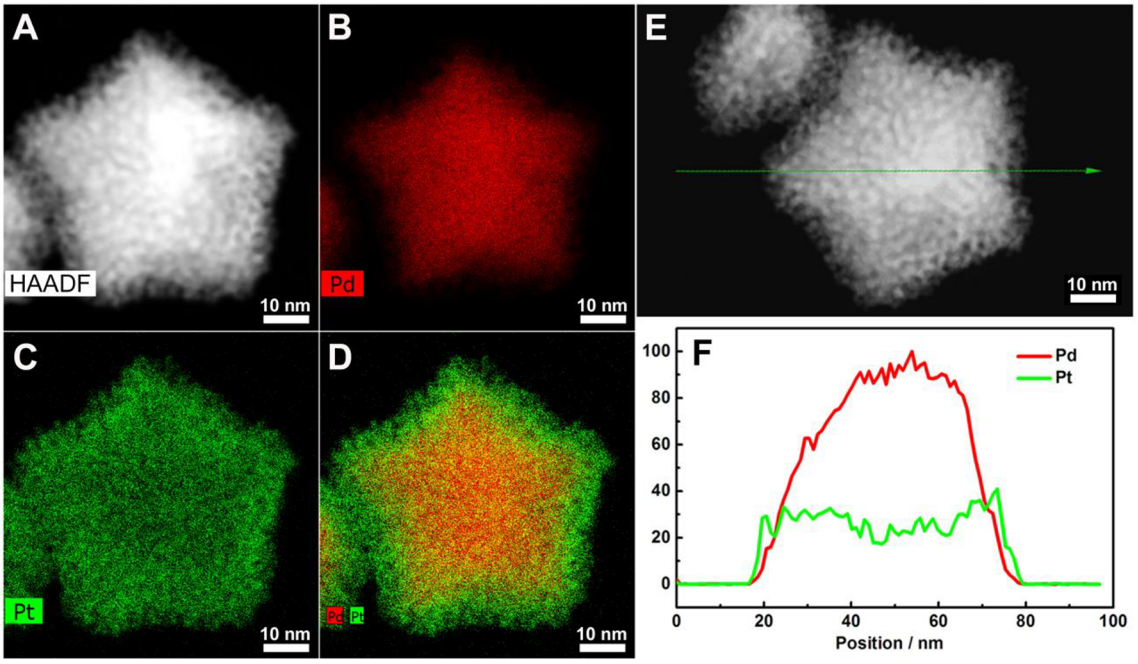

Figure 2. Compositional analyses of the Pd@PtNAs with 36.9 wt % Pt. (A) The HAADF-STEM image of Pd@PtNAs. The EDS elemental mapping of (B) Pd, (C) Pt, and their (D) overlapping image of Pd@PtNAs. (E) The HAADF-STEM image of Pd@PtNAs for EDS line-scan analysis. (F) The EDS line-scan analysis of Pd@PtNAs.

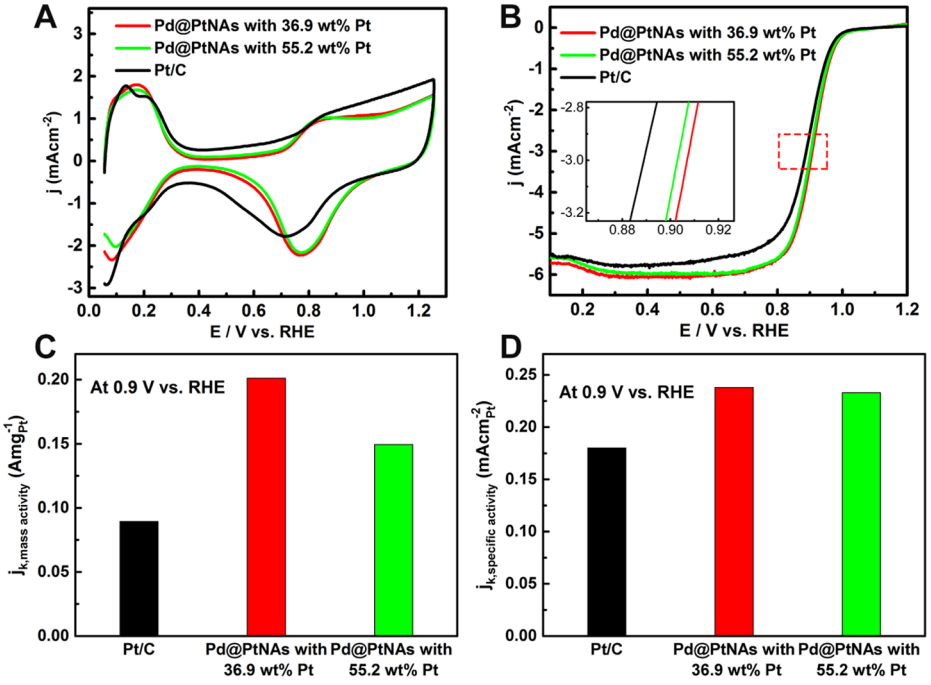

Figure 3. The electrochemical properties of electrocatalysts. (A) The CV curves of the catalysts. (B) The ORR polarization curves of the catalysts. The inset in (B) is the enlargement of the curve segments marked by the red-dashed frame. Mass (C) and specific (D) activities of the catalysts for ORR at 0.9 V versus RHE.

dispersed in the surface of decahedra. The EDS elemental mapping analysis showed the Pd decahedral core and Pt nanodots arrays shell (Figure 2B–D) in the Pd@PtNAs. These results were further confirmed by the EDS line-scan analysis (Figure 2E,F). The EDS pattern showed that Pd@PtNAs were composed of Pd and Pt (Figure S5).

In order to realize the influence of mass ratios of Pd/Pt on ORR activity, Pd@PtNAs with 36.9 and 55.2 wt % Pt were prepared by adding 88 and 176 μL H_2PtCl_6 (20 mM) solution under the same conditions (Table S1). Figure S6 showed TEM images of Pd@PtNAs with 36.9 and 55.2 wt % Pt. The sizes of Pd@PtNAs with 55.2 wt % Pt were 90–100 nm (Figure S6B), which was two more times larger than Pd@PtNAs with 36.9 wt % Pt (40–50 nm) (Figure S6A).

The catalytic activities of the Pd@PtNAs with 36.9 and 55.2 wt % Pt were evaluated toward ORR based on the commercial

DOI: 10.1021/acsanm.9b00610
ACS Appl. Nano Mater. 2019, 2, 3695–3700

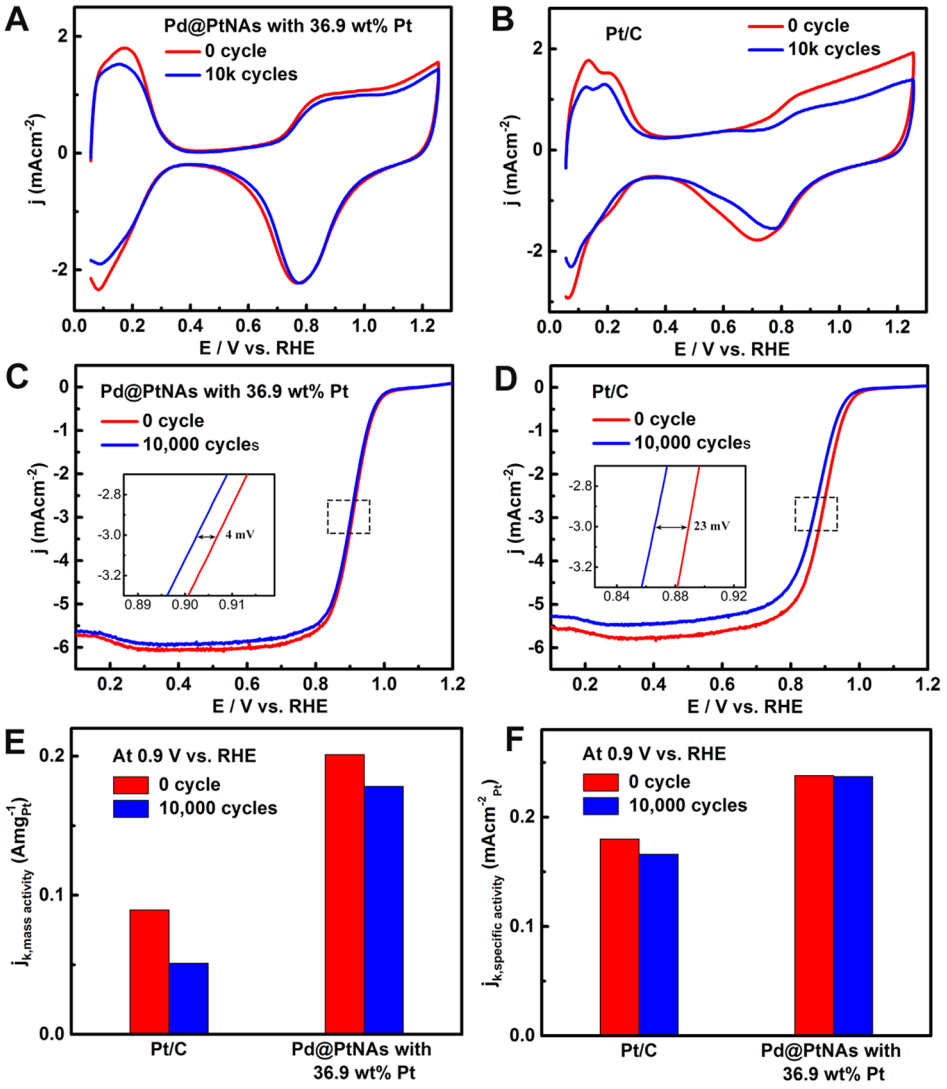

Figure 4. Electrochemical stability analysis of electrocatalysts. The CV curves (A,B) and ORR polarization curves (C,D) of the initial and 10 000 cycle potential sweeping of Pd@PtNAs with 36.9 wt % Pt and Pt/C, respectively. The inset in (C,D) is the magnification of the curve segments marked by the dark-dashed frame. Mass (E) and specific (F) activities of Pd@PtNAs with 36.9 wt % Pt and Pt/C for ORR at 0.9 V versus RHE in initial and 10 000 cycle of the stability tests.

Pt/C catalysts. Figure 3A showed typical CV curves of the as-prepared Pd@PtNAs and Pt/C at 25 °C in a N_2-saturated $HClO_4$ solution (0.1 M) with the sweeping rate of 50 mV/s between 0.056 and 1.256 V versus RHE (reversible hydrogen electrode). The Pd@PtNAs were wrapped with the Pt arrays which can be identified from the STEM-EDS mapping image (Figure 2). Therefore, the specific electrochemical active surface areas (ECSAs) of the catalysts were normalized to the Pt mass by hydrogen desorption. The ECSA of the catalysts were calculated by the charge required for the H_{upd} desorption between 0.056 and 0.35 V versus RHE in CV curves.[40] The specific ECSAs of both Pd@PtNAs were higher than that of Pt/C (Table S2, Figure S7). Especially, owing to a unique dispersion of Pt nanodot arrays on the surfaces of Pd decahedra, the specific ECSA of Pd@PtNAs with 36.9 wt % Pt was 84.38 m^2/g, which is better than that of Pt/C (49.64 m^2/g). The calculation method of ECSA here was similar to those in previously published literature.[11,18,23,26−28,41] Compared with these reports as shown in the Table S3, the ECSA of Pd@PtNAs was higher than part of them.[11,18,23,26−28,41] The Pd@PtNAs with 36.9 wt % Pt with a unique dispersion and smaller size (about 3 nm in diameter) of Pt nanodot arrays can greatly enhance the specific surface area of the catalyst. The result suggests that the specific surface area of Pt nanocrystals was significantly increased through forming nanodots arrays deposited on Pd decahedra. Meanwhile, the number of Pt atoms exposed to the surfaces was strikingly increased because of the ultrasmall size and high dispersion of Pt nanodots.[12,33,34]

Figure 3B shows the ORR polarization curves of the catalysts with an obvious positive-going result. The half-wave potentials of the Pd@PtNAs with 36.9 and 55.2 wt % Pt were 0.907 and 0.903 V versus RHE, showing 18 and 14 mV positive shift relatively to Pt/C (0.889 V) (Table S2). The Koutecky−Levich equation was used to calculate the mass activity and specific activity ($j_{k,mass}$, $j_{k,specific}$) of the Pd@PtNAs for ORR.[42] The $j_{k,mass}$ and $j_{k,specific}$ were normalized against the mass of Pt and ECSA.[42] The catalytic performance of the Pd@PtNAs with 36.9 and 55.2 wt % Pt was significantly improved in the potential region of 0.84−0.96 V versus RHE relative to Pt/C, and the Pd@PtNAs with 36.9 wt % Pt showed the strongest catalytic activities (Figure S8). At 0.9 V versus RHE, the $j_{k,mass}$ and $j_{k,specific}$ of the Pd@PtNAs with 36.9 wt % Pt were

DOI: 10.1021/acsanm.9b00610
ACS Appl. Nano Mater. 2019, 2, 3695−3700

0.20 A/mg_{Pt} and 0.24 mA/cm^2_{Pt}, which were 2.2 and 1.3 times that of the Pt/C (0.09 A/mg_{Pt} and 0.18 mA/cm^2_{Pt}), respectively (Figure 3C,D, Table S2). The distinguishingly branched structure of Pd@PtNAs provides a significantly high surface area of Pt despite the relatively large Pd particle size, which are beneficial to maximize the ORR performance of Pt.[27,30] In addition, the ultrasmall size Pt nanodots on the surface of Pd@PtNAs have abundant low-coordination atoms which are also favorable for improving its ORR activity.[43] All of these factors may enhance the catalytic activities of Pd@PtNAs for ORR.

The stability test of the Pd@PtNAs with 36.9 wt % Pt and Pt/C were conducted by accelerated durability test at 25 °C in an O_2-purged $HClO_4$ solution (0.1 M). Figure 4A,B shows CV curves of the initial and the 10 000 cycle potential sweeping of Pd@PtNAs with 36.9 wt % Pt and Pt/C, respectively. Both Pd@PtNAs with 36.9 wt % Pt and Pt/C had an attenuation in specific ECSA after 10 000 cycle stability tests (Figure S9). The specific ECSA of the Pd@PtNAs with 36.9 wt % Pt only decreased by 11%, while the ECSA of the Pt/C dropped by 38% (Figure S9). The half-wave potential of the Pd@PtNAs with 36.9 wt % Pt had a merely 4 mV negative shift (Figure 4C), whereas Pt/C had a 23 mV negative shift (Figure 4D) after 10 000 cycle stability tests. We calculated the activity of electrocatalysts for ORR after 10 000 cycle stability tests, finding that Pd@PtNAs with 36.9 wt % Pt had a slight loss of specific activity (0.4%) and mass activity (11.4%), compared with initial activity (Figure 4E,F). However, Pt/C had a larger loss of specific activity (7.8%) and mass activity (42.8%) relative to Pd@PtNAs with 36.9 wt % Pt (Figure 4E,F), respectively. It demonstrates that the Pd@PtNAs with 36.9 wt % Pt has a stable structure for ORR.

4. CONCLUSIONS

In summary, we found a facile and simple route for the direct synthesis of Pd@Pt core−shell nanodot array heterostructures in aqueous solution. Such ultrasmall size nanodot array structures remarkably increased the specific surface areas and activity of the catalysts, thus improving the utilization efficiency of Pt atoms in the process of electrocatalysis. Two species of Pd@PtNAs with different mass fractions of Pt were prepared toward the ORR. The Pd@PtNAs with 36.9 wt % Pt showed the highest activities. Compared with commercially available Pt/C catalysts, the mass activity at 0.9 V (versus RHE) of the Pd@PtNAs with 36.9 wt % Pt showed 2.2 times improvement for ORR. After 10 000 cycle of testing, the Pd@PtNAs with 36.9 wt % Pt had a slight loss of both mass activity (11.4%) and specific activity (0.4%). It reveals that Pd@PtNAs would readily improve the catalytic properties in both activity and durability. This method will effectively promote the one-step route to obtain nanostructures with nanodot arrays on the surface, which enhanced catalytic activities and the durability of catalysts.

■ ASSOCIATED CONTENT

Supporting Information

The Supporting Information is available free of charge on the ACS Publications website at DOI: 10.1021/acsanm.9b00610.

Additional characterization data, including EDS, XRD, TEM, ECSA, and catalytic performance; photographs of experiment; data tables; and equation information (PDF)

■ AUTHOR INFORMATION

Corresponding Author

*E-mail: hyhan@mail.hzau.edu.cn. Tel: +86-27-87282043.

ORCID

Heyou Han: 0000-0001-9406-0722

Notes

The authors declare no competing financial interest.

■ ACKNOWLEDGMENTS

This work was financially supported by National Key R&D Program of China (2016YFD0500706), National Natural Science Foundation of China (21778020) and Sci-tech Innovation Foundation of Huazhong Agriculture University (2662017PY042, 2662018PY024). We thank Jianbo Cao and Limin He for their help with part of the TEM testing at Huazhong Agricultural University (HZAU).

■ REFERENCES

(1) Liu, J.; Zheng, Y.; Hong, Z.; Cai, K.; Zhao, F.; Han, H. Microbial Synthesis of Highly Dispersed PdAu Alloy for Enhanced Electrocatalysis. *Sci. Adv.* **2016**, *2*, No. e1600858.

(2) Wang, Y.-J.; Wilkinson, D. P.; Zhang, J. Noncarbon Support Materials for Polymer Electrolyte Membrane Fuel Cell Electrocatalysts. *Chem. Rev.* **2011**, *111*, 7625−7651.

(3) Nie, Y.; Li, L.; Wei, Z. Recent Advancements in Pt and Pt-Free Catalysts for Oxygen Reduction Reaction. *Chem. Soc. Rev.* **2015**, *44*, 2168−2201.

(4) Porter, N. S.; Wu, H.; Quan, Z.; Fang, J. Shape-Control and Electrocatalytic Activity-Enhancement of Pt-Based Bimetallic Nanocrystals. *Acc. Chem. Res.* **2013**, *46*, 1867−1877.

(5) Wu, J.; Yang, H. Platinum-Based Oxygen Reduction Electrocatalysts. *Acc. Chem. Res.* **2013**, *46*, 1848−1857.

(6) Peng, Z.; Yang, H. Designer Platinum Nanoparticles: Control of Shape, Composition in Alloy, Nanostructure and Electrocatalytic Property. *Nano Today* **2009**, *4*, 143−164.

(7) Wang, Y. J.; Zhao, N.; Fang, B.; Li, H.; Bi, X. T.; Wang, H. Carbon-Supported Pt-Based Alloy Electrocatalysts for the Oxygen Reduction Reaction in Polymer Electrolyte Membrane Fuel Cells: Particle Size, Shape, and Composition Manipulation and their Impact to Activity. *Chem. Rev.* **2015**, *115*, 3433−3467.

(8) Li, M.; Zhao, Z.; Cheng, T.; Fortunelli, A.; Chen, C.-Y.; Yu, R.; Zhang, Q.; Gu, L.; Merinov, B.; Lin, Z.; Zhu, E.; Yu, T.; Jia, Q.; Guo, J.; Zhang, L.; Goddard III, W. A.; Huang, Y.; Duan, X. Ultrafine Jagged Platinum Nanowires Enable Ultrahigh Mass Activity for the Oxygen Reduction Reaction. *Science* **2016**, *354*, 1414−1419.

(9) Choi, R.; Choi, S. I.; Choi, C. H.; Nam, K. M.; Woo, S. I.; Park, J. T.; Han, S. W. Designed Synthesis of Well-Defined Pd@Pt Core-Shell Nanoparticles with Controlled Shell Thickness as Efficient Oxygen Reduction Electrocatalysts. *Chem. - Eur. J.* **2013**, *19*, 8190−8198.

(10) Zhao, R.; Liu, Y.; Liu, C.; Xu, G.; Chen, Y.; Tang, Y.; Lu, T. Pd@Pt Core-Shell Tetrapods as Highly Active and Stable Electrocatalysts for the Oxygen Reduction Reaction. *J. Mater. Chem. A* **2014**, *2*, 20855−20860.

(11) Zhang, L.; Roling, L. T.; Wang, X.; Vara, M.; Chi, M.; Liu, J.; Choi, S.-II.; Park, J.; Herron, J. A.; Xie, Z.; Mavrikakis, M.; Xia, Y. Platinum-Based Nanocages with Subnanometer-Thick Walls and Well-Defined, Controllable Facets. *Science* **2015**, *349*, 412−416.

(12) Ma, Y.; Gao, W.; Shan, H.; Chen, W.; Shang, W.; Tao, P.; Song, C.; Addiego, C.; Deng, T.; Pan, X.; Wu, J. Platinum-Based Nanowires as Active Catalysts toward Oxygen Reduction Reaction: In Situ Observation of Surface-Diffusion-Assisted, Solid-State Oriented Attachment. *Adv. Mater.* **2017**, *29*, 1703460.

(13) Zuo, Y.; Cai, K.; Wu, L.; Li, T.; Lv, Z.; Liu, J.; Shao, K.; Han, H. Spiny-Porous Platinum Nanotubes with Enhanced Electrocatalytic

DOI: 10.1021/acsanm.9b00610
ACS Appl. Nano Mater. 2019, 2, 3695−3700

Activity for Methanol Oxidation. *J. Mater. Chem. A* **2015**, *3*, 1388−1391.
(14) Zuo, Y.; Li, T.; Ren, H.; Zhu, G.; Han, K.; Zhuang, L.; Han, H. Self-Assembly of Pt-Based Truncated Octahedral Crystals into Metal-Frameworks towards Enhanced Electrocatalytic Activity. *J. Mater. Chem. A* **2016**, *4*, 15169−15180.
(15) Park, J.; Mrinal, K. K.; Kwon, H.; Park, S.; Baik, H.; Choi, S.-Il.; Lee, K. Radially Phase Segregated PtCu@PtCuNi Dendrite@Frame Nanocatalyst for the Oxygen Reduction Reaction. *ACS Nano* **2017**, *11*, 10844−10851.
(16) Zuo, Y.; Wu, L.; Cai, K.; Li, T.; Yin, W.; Li, D.; Li, N.; Liu, J.; Han, H. Platinum Dendritic-Flowers Prepared by Tellurium Nanowires Exhibit High Electrocatalytic Activity for Glycerol Oxidation. *ACS Appl. Mater. Interfaces* **2015**, *7*, 17725−17730.
(17) Chen, Y.; Yang, J.; Yang, Y.; Peng, Z.; Li, J.; Mei, T.; Wang, J.; Hao, M.; Chen, Y.; Xiong, W.; Zhang, L.; Wang, X. A Facile Strategy to Synthesize Three-Dimensional Pd@Pt Core-Shell Nanoflowers Supported on Graphene Nanosheets as Enhanced Nanoelectrocatalysts for Methanol Oxidation. *Chem. Commun.* **2015**, *51*, 10490−10493.
(18) Wang, W.; Zhao, Y.; Ding, Y. 2D Ultrathin Core-Shell Pd@$Pt_{monolayer}$Nanosheets: Defect-Mediated Thin Film Growth and Enhanced Oxygen Reduction Performance. *Nanoscale* **2015**, *7*, 11934−11939.
(19) Koenigsmann, C.; Santulli, A. C.; Gong, K.; Vukmirovic, M. B.; Zhou, W. P.; Sutter, E.; Wong, S. S.; Adzic, R. R. Enhanced Electrocatalytic Performance of Processed, Ultrathin, Supported Pd-Pt Core-Shell Nanowire Catalysts for the Oxygen Reduction Reaction. *J. Am. Chem. Soc.* **2011**, *133*, 9783−9795.
(20) Li, H. H.; Ma, S. Y.; Fu, Q. Q.; Liu, X. J.; Wu, L.; Yu, S. H. Scalable Bromide-Triggered Synthesis of Pd@Pt Core-Shell Ultrathin Nanowires with Enhanced Electrocatalytic Performance toward Oxygen Reduction Reaction. *J. Am. Chem. Soc.* **2015**, *137*, 7862−7868.
(21) Xiong, Y.; Shan, H.; Zhou, Z.; Yan, Y.; Chen, W.; Yang, Y.; Liu, Y.; Tian, H.; Wu, J.; Zhang, H.; Yang, D. Tuning Surface Structure and Strain in Pd-Pt Core-Shell Nanocrystals for Enhanced Electrocatalytic Oxygen Reduction. *Small* **2017**.
(22) Peng, Z.; Yang, H. Synthesis and Oxygen Reduction Electrocatalytic Property of Pt-on-Pd Bimetallic Heteronanostructures. *J. Am. Chem. Soc.* **2009**, *131*, 7542−7543.
(23) Park, J.; Zhang, L.; Choi, S.-I.; Roling, L. T.; Lu, N.; Herron, J. A.; Xie, S.; Wang, J.; Kim, M. J.; Mavrikakis, M.; Xia, Y. Atomic Layer-by-Layer Deposition of Platinum on Palladium Octahedra for Enhanced Catalysts toward the Oxygen Reduction Reaction. *ACS Nano* **2015**, *9*, 2635−2647.
(24) Park, J.; Vara, M.; Xia, Y. A Systematic Study of the Catalytic Durability of Pd@Pt_{2-3L}Nano-Sized Octahedra toward Oxygen Reduction. *Catal. Today* **2017**, *280*, 266−273.
(25) Zhou, M.; Wang, H.; Elnabawy, A. O.; Hood, Z. D.; Chi, M.; Xiao, P.; Zhang, Y.; Mavrikakis, M.; Xia, Y. Facile One-Pot Synthesis of Pd@Pt_{1L} Octahedra with Enhanced Activity and Durability toward Oxygen Reduction. *Chem. Mater.* **2019**, *31*, 1370−1380.
(26) Wang, X.; Vara, M.; Luo, M.; Huang, H.; Ruditskiy, A.; Park, J.; Bao, S.; Liu, J.; Howe, J.; Chi, M.; Xie, Z.; Xia, Y. Pd@Pt Core-Shell Concave Decahedra: A Class of Catalysts for the Oxygen Reduction Reaction with Enhanced Activity and Durability. *J. Am. Chem. Soc.* **2015**, *137*, 15036−15042.
(27) Xie, S.; Choi, S.-I.; Lu, N.; Roling, L. T.; Herron, J. A.; Zhang, L.; Park, J.; Wang, J.; Kim, M. J.; Xie, Z.; Mavrikakis, M.; Xia, Y. Atomic Layer-by-Layer Deposition of Pt on Pd Nanocubes for Catalysts with Enhanced Activity and Durability toward Oxygen Reduction. *Nano Lett.* **2014**, *14*, 3570−3576.
(28) Wang, X.; Choi, S.-I.; Roling, L. T.; Luo, M.; Ma, C.; Zhang, L.; Chi, M.; Liu, J.; Xie, Z.; Herron, J. A.; Mavrikakis, M.; Xia, Y. Palladium-Platinum Core-Shell Icosahedra with Substantially Enhanced Activity and Durability towards Oxygen Reduction. *Nat. Commun.* **2015**, *6*, 7594.
(29) Lee, C. T.; Wang, H.; Zhao, M.; Yang, T. H.; Vara, M.; Xia, Y. One-Pot Synthesis of Pd@PtnL Core-Shell Icosahedral Nanocrystals in High Throughput through a Quantitative Analysis of the Reduction Kinetics. *Chem. - Eur. J.* **2019**, *25*, 5322−5329.
(30) Lim, B.; Jiang, M.; Camargo, P. H. C.; Cho, E. C.; Tao, J.; Lu, X.; Zhu, Y.; Xia, Y. Pd-Pt Bimetallic Nanodendrites with High Activity for Oxygen Reduction. *Science* **2009**, *324*, 1302−1305.
(31) Wang, L.; Nemoto, Y.; Yamauchi, Y. Direct Synthesis of Spatially-Controlled Pt-on-Pd Bimetallic Nanodendrites with Superior Electrocatalytic Activity. *J. Am. Chem. Soc.* **2011**, *133*, 9674−9677.
(32) Wang, L.; Yamauchi, Y. Metallic Nanocages: Synthesis of Bimetallic Pt-Pd Hollow Nanoparticles with Dendritic Shells by Selective Chemical Etching. *J. Am. Chem. Soc.* **2013**, *135*, 16762−16765.
(33) Siburian, R.; Kondo, T.; Nakamura, J. Size Control to a Sub-Nanometer Scale in Platinum Catalysts on Graphene. *J. Phys. Chem. C* **2013**, *117*, 3635−3645.
(34) Chen, C.; Kang, Y.; Huo, Z.; Zhu, Z.; Huang, W.; Xin, H. L.; Snyder, J. D.; Li, D.; Herron, J. A.; Mavrikakis, M.; Chi, M.; More, K. L.; Li, Y.; Markovic, N. M.; Somorjai, G. A.; Yang, P.; Stamenkovic, V. R. Highly Crystalline Multimetallic Nanoframes with Three-Dimensional Electrocatalytic Surfaces. *Science* **2014**, *343*, 1339−1343.
(35) Chen, Y.; Fan, Z.; Luo, Z.; Liu, X.; Lai, Z.; Li, B.; Zong, Y.; Gu, L.; Zhang, H. High-Yield Synthesis of Crystal-Phase-Heterostructured 4H/fcc Au@Pd Core-Shell Nanorods for Electrocatalytic Ethanol Oxidation. *Adv. Mater.* **2017**, *29*, 1701331.
(36) Hong, J. W.; Kang, S. W.; Choi, B.-S.; Kim, D.; Lee, S. B.; Han, S. W. Controlled Synthesis of Pd-Pt Alloy Hollow Nanostructures with Enhanced Catalytic Activities for Oxygen Reduction. *ACS Nano* **2012**, *6*, 2410−2419.
(37) Guo, J.; Zhang, Y.; Shi, L.; Zhu, Y.; Mideksa, M. F.; Hou, K.; Zhao, W.; Wang, D.; Zhao, M.; Zhang, X.; Lv, J.; Zhang, J.; Wang, X.; Tang, Z. Boosting Hot Electrons in Hetero-Superstructures for Plasmon-Enhanced Catalysis. *J. Am. Chem. Soc.* **2017**, *139*, 17964−17972.
(38) Zuo, Y.; Rao, D.; Li, S.; Li, T.; Zhu, G.; Chen, S.; Song, L.; Chai, Y.; Han, H. Atomic Vacancies Control of Pd-Based Catalysts for Enhanced Electrochemical Performance. *Adv. Mater.* **2018**, *30*, 1704171.
(39) Zhang, H.; Yin, Y.; Hu, Y.; Li, C.; Wu, P.; Wei, S.; Cai, C. Pd@Pt Core-Shell Nanostructures with Controllable Composition Synthesized by a Microwave Method and Their Enhanced Electrocatalytic Activity toward Oxygen Reduction and Methanol Oxidation. *J. Phys. Chem. C* **2010**, *114*, 11861−11867.
(40) He, D.; Zhang, L.; He, D.; Zhou, G.; Lin, Y.; Deng, Z.; Hong, X.; Wu, Y.; Chen, C.; Li, Y. Amorphous Nickel Boride Membrane on a Platinum-Nickel Alloy Surface for Enhanced Oxygen Reduction Reaction. *Nat. Commun.* **2016**, *7*, 12362.
(41) He, D. S.; He, D.; Wang, J.; Lin, Y.; Yin, P.; Hong, X.; Wu, Y.; Li, Y. Ultrathin Icosahedral Pt-Enriched Nanocage with Excellent Oxygen Reduction Reaction Activity. *J. Am. Chem. Soc.* **2016**, *138*, 1494−1497.
(42) Treimer, S.; Tang, A.; Johnson, D. C. Consideration of the Application of Koutecky-Levich Plots in the Diagnoses of Charge-Transfer Mechanisms at Rotated Disk Electrodes. *Electroanalysis* **2002**, *14*, 165−171.
(43) Zhang, X.; Guan, P.; Malic, L.; Trudeau, M.; Rosei, F.; Veres, T. Nanoporous Twinned PtPd with Highly Catalytic Activity and Stability. *J. Mater. Chem. A* **2015**, *3*, 2050−2056.

DOI: 10.1021/acsanm.9b00610
ACS Appl. Nano Mater. 2019, 2, 3695−3700